



Crystal structure of a new tripotassium hexanickel iron hexaphosphate

Said Ouaatta,* Abderrazzak Assani, Mohamed Saadi and Lahcen El Ammari

Laboratoire de Chimie Appliquée des Matériaux, Centre des Sciences des Matériaux, Faculty of Sciences, Mohammed V University in Rabat, Avenue Ibn Batouta, BP 1014, Rabat, Morocco. *Correspondence e-mail: saidouaatta87@gmail.com

Received 18 February 2019

Accepted 21 February 2019

Edited by A. Van der Lee, Université de Montpellier II, France

Keywords: crystal structure; crystal growth; β -xenophyllite structure; $K_3Ni_6Fe(PO_4)_6$; X-ray diffraction; othophosphate; solid-state reaction synthesis.

CCDC reference: 1898755

Supporting information: this article has supporting information at journals.iucr.org/e

A new potassium-nickel iron phosphate, $K_3Ni_6Fe(PO_4)_6$, has been synthesized by solid-state reaction and structurally characterized by single-crystal X-ray diffraction and qualitative energy dispersive X-ray spectroscopy (EDS) analysis. The structure is built up by $[FeO_6]$, $[PO_4]$, and $[NiO_6]$ coordination polyhedra, which are linked to each other by edge and corner sharing to form zigzag layers parallel to the ab plane. These layers are interconnected by $[PO_4]$ tetrahedra and $[NiO_6]$ octahedra *via* common corners, leading to a three-dimensional framework delimiting large channels running along the $[100]$ direction in which the K^+ cations are localized.

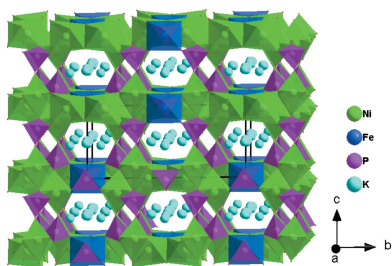
1. Chemical context

Iron-based phosphates are widely studied materials today. They present a promising field for various applications such as electronics (Saw *et al.*, 2014), ferroelectrics (Lazoryak *et al.*, 2004), magnetic materials (Hatert *et al.*, 2004; Essehli *et al.*, 2015) and catalytic processes (Moffat, 1978). The introduction of alkali metals into these phosphates materials can be of great interest to improve the ion-conduction properties for applications in rechargeable alkaline batteries (La Parola *et al.*, 2018; Orikasa *et al.*, 2016). The present work is part of our activity devoted particularly to the investigation of new materials based on phosphates belonging to the $A_2O-MO-Fe_2O_3-P_2O_5$ (A = an alkali metal; M = divalent cation) quaternary system, which could have interesting ionic conductivity or magnetic properties. We report herein on the synthesis and structural characterization by single crystal X-ray diffraction of a new potassium nickel iron phosphate with formula $K_3Ni_6Fe(PO_4)_6$.

2. Structural commentary

The asymmetric unit of the title compound, $K_3Ni_6Fe(PO_4)_6$, consists of two $[NiO_6]$ octahedra, one $[FeO_6]$ octahedron, two $[PO_4]$ tetrahedra, and three K atoms, as shown in Fig. 1. One Ni^{2+} , Fe^{3+} , P^{5+} , two K^+ cations and two of the seven oxygen atoms lie on special positions. The Ni2 atom occupies Wyckoff position 4g (2), the Fe atom is localized on the 2a (2/m) Wyckoff position, P2, K1, K3, O6 and O7 are positioned on 4i (m) sites. The octahedral coordination sphere of the nickel(II) cation

is more distorted than that of the iron(III) atom, with average $\langle Ni-O \rangle$ distances of 2.066 and 2.119 Å for Ni1 and Ni2, respectively. The mean $\langle P-O \rangle$ distance in the two PO_4 tetrahedra is equal to 1.547 Å for P1 and 1.543 Å for P2.



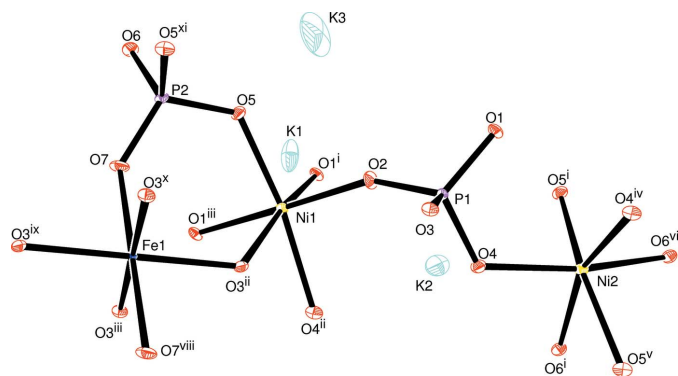


Figure 1
Molecular structure of the title compound with the atom-labelling scheme. Displacement ellipsoids are drawn at the 50% probability level. Symmetry codes: (i) $-x + \frac{1}{2}, -y + \frac{3}{2}, -z + 1$; (ii) $-x + 1, y, -z + 1$; (iii) $x, y, z - 1$; (iv) $-x + 1, y, -z + 2$; (v) $x + \frac{1}{2}, -y + \frac{3}{2}, z + 1$; (vi) $x + \frac{1}{2}, y + \frac{1}{2}, z + 1$; (vii) $-x + 1, -y + 1, -z$; (viii) $x, -y + 1, z - 1$; (ix) $-x + 1, -y + 1, -z + 1$; (x) $x, -y + 1, z$; (xi) $x, y, z + 1$; (xii) $-x + \frac{1}{2}, -y + \frac{3}{2}, -z$; (xiii) $-x, -y + 1, -z$; (xiv) $x, -y + 2, z$.

The Fe atoms are coordinated octahedrally with an average $\langle \text{Fe}-\text{O} \rangle$ distance of 2.038 Å. The structure of the title compound is built up from two types of nickel sites and one iron site, each with an octahedral coordination environment, $[\text{Ni}_1\text{O}_6]$, $[\text{Ni}_2\text{O}_6]$ and $[\text{FeO}_6]$, besides two independent phosphor tetrahedra $[\text{P}1\text{O}_4]$ and $[\text{P}2\text{O}_4]$. Edge-sharing $[\text{Ni}_2\text{O}_6]$ octahedra build up a dimeric $[\text{Ni}_2\text{O}_{10}]$ unit. Two $[\text{P}2\text{O}_6]$ octahedra are connected to the $[\text{Ni}_2\text{O}_{10}]$ dimer by sharing edges to form an $[\text{Ni}(2)_2\text{P}(2)_2\text{O}_{12}]$ unit, which alternates with an $[\text{FeO}_6]$ octahedron to establish an infinite chain along the $[100]$ direction (Fig. 2). In addition, the association between the $[\text{P}1\text{O}_4]$ tetrahedra and the $[\text{Ni}_1\text{O}_6]$ octahedra by means of edge-sharing allows the formation of a zigzag chain running parallel to the $[100]$ direction. Each of the $\text{P}1\text{O}_4$ tetrahedra

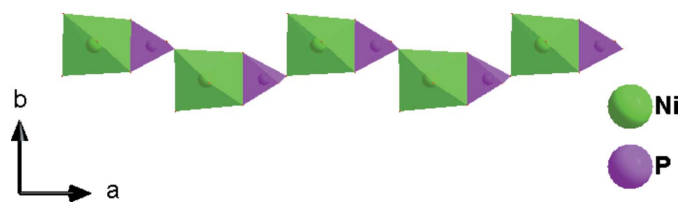


Figure 3
Corner- and edge-sharing $[\text{P}1\text{O}_4]$ tetrahedra and $[\text{Ni}_1\text{O}_6]$ octahedra forming a zigzag shape chain running parallel to $[100]$

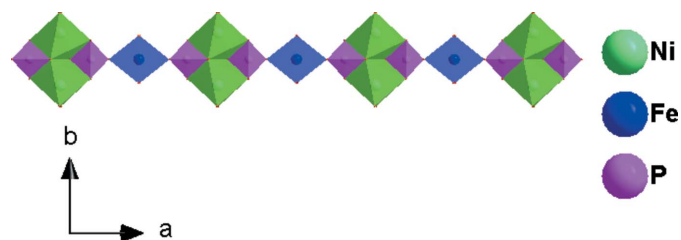


Figure 2
A chain formed by sharing edges and corners of $[\text{Ni}_2\text{O}_{10}]$ dimers, $[\text{P}2\text{O}_4]$ tetrahedra and $[\text{FeO}_6]$ octahedra along the $[100]$ direction

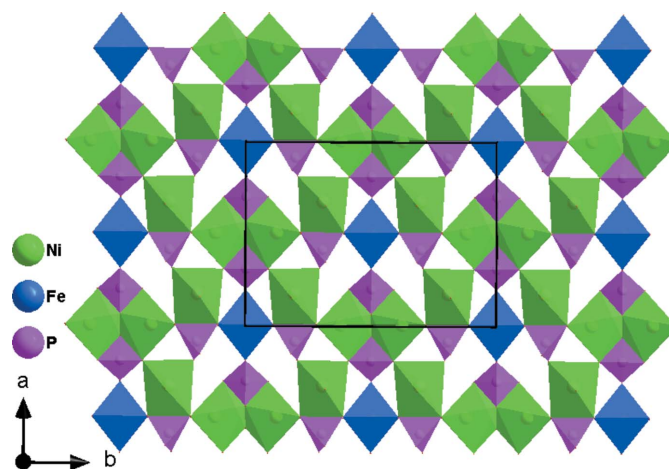


Figure 4
View along the c axis of corner- and edge-sharing $[\text{PO}_4]$ tetrahedra and $[\text{NiO}_6]$ octahedra forming a layer parallel to the ab plane.

and Ni_1O_6 octahedra, both belonging to the same layer, share vertices with Ni_1O_6 and $\text{P}1\text{O}_4$, respectively, of the adjacent one (Fig. 3). The two types of chain linkages lead to the formation of layers parallel to the ab plane (Fig. 4). One vertex of an Ni_1O_6 octahedron belonging to one layer is shared with a $\text{P}1\text{O}_4$ vertex of the neighbouring layer. This configuration leads to a three-dimensional centrosymmetric framework, delimiting hexagonal tunnels along the $[100]$ direction, in which the K^+ cations are located (Fig. 5). The potassium cations are distributed over three independent crystallographic positions with partial occupancies

3. Database survey

The investigated compound is a new member of the β -xenophyllite family that includes $\text{Na}_4\text{Ni}_7(\text{PO}_4)_6$ (Moring & Kostiner, 1986), $\text{Na}_4\text{Co}_7(\text{PO}_4)_6$ (Kobashi *et al.*, 1998),

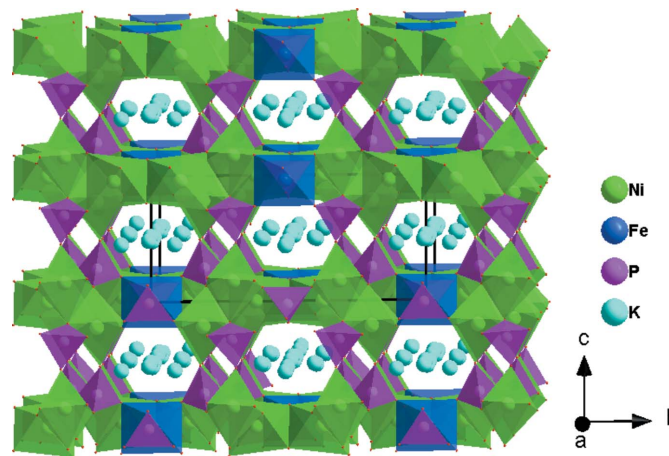


Figure 5
Polyhedral representation of the crystal structure of $\text{K}_3\text{Ni}_6\text{Fe}(\text{PO}_4)_6$ showing large tunnels running along the $[100]$ direction that contain the K^+ cations.

Table 1
Experimental details.

Crystal data	
Chemical formula	$K_3Ni_6Fe(PO_4)_6$
M_r	1095.23
Crystal system, space group	Monoclinic, $C2/m$
Temperature (K)	296
a, b, c (Å)	10.6853 (4), 14.1009 (5), 6.5481 (2)
β (°)	103.842 (1)
V (Å ³)	957.97 (6)
Z	2
Radiation type	Mo $K\alpha$
μ (mm ⁻¹)	7.79
Crystal size (mm)	0.36 × 0.27 × 0.20
Data collection	
Diffractometer	Bruker D8 VENTURE Super DUO
Absorption correction	Multi-scan (<i>SADABS</i> ; Krause <i>et al.</i> , 2015)
T_{min}, T_{max}	0.638, 0.746
No. of measured, independent and observed [$I > 2\sigma(I)$] reflections	13870, 1981, 1891
R_{int}	0.021
$(\sin \theta/\lambda)_{max}$ (Å ⁻¹)	0.781
Refinement	
$R[F^2 > 2\sigma(F^2)], wR(F^2), S$	0.024, 0.062, 1.07
No. of reflections	1981
No. of parameters	112
$\Delta\rho_{max}, \Delta\rho_{min}$ (e Å ⁻³)	2.34, -1.16

Computer programs: *APEX3* and *SAINT-Plus* (Bruker, 2016), *SHELXT2014* (Sheldrick, 2015a), *SHELXL2016* (Sheldrick, 2015b), *ORTEP-3 for Windows* (Farrugia, 2012), *DIAMOND* (Brandenburg, 2006) and *publCIF* (Westrip, 2010).

$K_4Ni_7(AsO_4)_6$ (Ben Smail *et al.*, 1999), $Na_4Co_{5.63}Al_{0.91}(AsO_4)_6$ (Marzouki *et al.*, 2010), $Na_4Li_{0.62}Co_{5.67}Al_{0.71}(AsO_4)_6$ (Marzouki *et al.*, 2013), $Ag_4Co_7(AsO_4)_6$ (Marzouki *et al.*, 2014) and $Na_4Co_7(AsO_4)_6$ (Ben Smida *et al.*, 2016). The phosphates of these compounds crystallize in the non-centrosymmetric Cm space group while the arsenates adopt the $C2/m$ space group.

4. Synthesis and crystallization

Single crystals of $K_3Ni_6Fe(PO_4)_6$ were prepared by solid-state reaction in air. A mixture of K_2CO_3 , $Ni(NO_3)_2 \cdot 6H_2O$, $Fe(NO_3)_3 \cdot 9H_2O$ and H_3PO_4 (85 wt.%) reagents with a K:Ni:Fe:P molar ratio of 2:2:1:3 was dissolved in 50 mL of distilled water. The resulting solution was stirred without heating for 24 h and was subsequently evaporated to dryness at 343 K. The obtained dry residue was progressively heated in a platinum crucible up to 673 K in order to eliminate volatile products. In a second step, the powder was homogenized in an agate mortar and then progressively heated to 1303 K. Kept at this temperature for 2 h, the reaction mixture then underwent slow cooling at a rate of 5 K h⁻¹ to 1103 K and then to room temperature with the furnace inertia. After washing with distilled water, the obtained crystals were brown with block-

type shape. A qualitative EDX analysis (energy dispersive X-ray spectroscopy) detected the presence of the expected chemical elements corresponding to K, Ni, Fe, P and O atoms (see Fig. 6).

5. Refinement

Crystal data, data collection and structure refinement details of $K_3Ni_6Fe(PO_4)_6$ are summarized in Table 1. The highest peak and the deepest hole in the final Fourier map are at 0.71 and 0.59 Å, respectively, from atom K2.

Acknowledgements

The authors thank the Faculty of Science of the Mohammed V University in Rabat, Morocco, for the X-ray measurements.

References

- Ben Smail, R., Driss, A. & Jouini, T. (1999). *Acta Cryst.* **C55**, 284–286.
- Ben Smida, Y., Marzouki, R., Georges, S., Kutteh, R., Avdeev, M., Guesmi, A. & Zid, M. F. (2016). *J. Solid State Chem.* **239**, 8–16.
- Brandenburg, K. (2006). *DIAMOND*. Crystal Impact GbR, Bonn, Germany.
- Bruker (2016). *APEX3, SAINT-Plus* and *SADABS*. Bruker AXS Inc., Madison, Wisconsin, USA.
- Essehli, R., Belharouak, I., Ben Yahia, H., Chamoun, R., Orayech, B., El Bali, B., Bouziane, K., Zhou, X. L. & Zhou, Z. (2015). *Dalton Trans.* **44**, 4526–4532.
- Farrugia, L. J. (2012). *J. Appl. Cryst.* **45**, 849–854.
- Hatert, F., Long, G. J., Hautot, D., Fransolet, A. M., Delwiche, J., Hubin-Franskin, M. J. & Grandjean, F. (2004). *Phys. Chem. Miner.* **31**, 487–506.
- Kobashi, D., Kohara, S., Yamakawa, J. & Kawahara, A. (1998). *Acta Cryst.* **C54**, 7–9.
- Krause, L., Herbst-Irmer, R., Sheldrick, G. M. & Stalke, D. (2015). *J. Appl. Cryst.* **48**, 3–10.
- La Parola, V., Liveri, V. T., Todaro, L., Lombardo, D., Bauer, E. M., Dell’Era, A., Longo, A., Caschera, D., de Caro, T., Toro, R. G. & Calandra, P. (2018). *Mater. Lett.* **220**, 58–61.
- Lazoryak, B. I., Morozov, V. A., Belik, A. A., Stefanovich, S. Y., Grebenev, V. V., Leonidov, I. A., Mitberg, E. B., Davydov, S. A., Lebedev, O. I. & Van Tendeloo, G. (2004). *Solid State Sci.* **6**, 185–195.
- Marzouki, R., Frigui, W., Guesmi, A., Zid, M. F. & Driss, A. (2013). *Acta Cryst.* **E69**, i65–i66.
- Marzouki, R., Guesmi, A. & Driss, A. (2010). *Acta Cryst.* **C66**, i95–i98.
- Marzouki, R., Guesmi, A., Georges, S., Zid, M. F. & Driss, A. (2014). *J. Alloys Compd.* **586**, 74–79.
- Moffat, J. B. (1978). *Catal. Rev.* **18**, 199–258.
- Moring, J. & Kostiner, E. (1986). *J. Solid State Chem.* **62**, 105–111.
- Orikasa, Y., Gogyo, Y., Yamashige, H., Katayama, M., Chen, K., Mori, T., Yamamoto, K., Masese, T., Inada, Y., Ohta, T., Siroma, Z., Kato, S., Kinoshita, H., Arai, H., Ogumi, Z. & Uchimoto, Y. (2016). *Sci. Rep.* **6**, article No. 26382.
- Saw, L. H., Somasundaram, K., Ye, Y. & Tay, A. A. O. (2014). *J. Power Sources*, **249**, 231–238.
- Sheldrick, G. M. (2015a). *Acta Cryst.* **A71**, 3–8.
- Sheldrick, G. M. (2015b). *Acta Cryst.* **C71**, 3–8.
- Westrip, S. P. (2010). *J. Appl. Cryst.* **43**, 920–925.

supporting information

Acta Cryst. (2019). E75, 402-404 [https://doi.org/10.1107/S2056989019002706]

Crystal structure of a new tripotassium hexanickel iron hexaphosphate

Said Ouatta, Abderrazzak Assani, Mohamed Saadi and Lahcen El Ammari

Computing details

Data collection: *APEX3* (Bruker, 2016); cell refinement: *SAINTE-Plus* (Bruker, 2016); data reduction: *SAINTE-Plus* (Bruker, 2016); program(s) used to solve structure: *SHELXT2014* (Sheldrick, 2015a); program(s) used to refine structure: *SHELXL2016* (Sheldrick, 2015b); molecular graphics: *ORTEP-3 for Windows* (Farrugia, 2012) and *DIAMOND* (Brandenburg, 2006); software used to prepare material for publication: *publCIF* (Westrip, 2010).

Tripotassium hexanickel iron hexaphosphate

Crystal data

$\text{K}_3\text{Ni}_6\text{Fe}(\text{PO}_4)_6$

$M_r = 1095.23$

Monoclinic, *C2/m*

$a = 10.6853$ (4) Å

$b = 14.1009$ (5) Å

$c = 6.5481$ (2) Å

$\beta = 103.842$ (1)°

$V = 957.97$ (6) Å³

$Z = 2$

$F(000) = 1066$

$D_x = 3.797$ Mg m⁻³

Mo $K\alpha$ radiation, $\lambda = 0.71073$ Å

Cell parameters from 1981 reflections

$\theta = 2.4\text{--}33.7^\circ$

$\mu = 7.79$ mm⁻¹

$T = 296$ K

Block, brown

$0.36 \times 0.27 \times 0.20$ mm

Data collection

Bruker D8 VENTURE Super DUO
diffractometer

Radiation source: INCOATEC I μ S micro-focus
source

HELIOS mirror optics monochromator

Detector resolution: 10.4167 pixels mm⁻¹

φ and ω scans

Absorption correction: multi-scan
(SADABS; Krause *et al.*, 2015)

$T_{\min} = 0.638$, $T_{\max} = 0.746$

13870 measured reflections

1981 independent reflections

1891 reflections with $I > 2\sigma(I)$

$R_{\text{int}} = 0.021$

$\theta_{\max} = 33.7^\circ$, $\theta_{\min} = 2.4^\circ$

$h = -14 \rightarrow 16$

$k = -22 \rightarrow 22$

$l = -10 \rightarrow 10$

Refinement

Refinement on F^2

Least-squares matrix: full

$R[F^2 > 2\sigma(F^2)] = 0.024$

$wR(F^2) = 0.062$

$S = 1.07$

1981 reflections

112 parameters

0 restraints

$w = 1/[\sigma^2(F_o^2) + (0.0262P)^2 + 6.1957P]$

where $P = (F_o^2 + 2F_c^2)/3$

$(\Delta/\sigma)_{\max} = 0.001$

$\Delta\rho_{\max} = 2.34$ e Å⁻³

$\Delta\rho_{\min} = -1.16$ e Å⁻³

Special details

Geometry. All esds (except the esd in the dihedral angle between two l.s. planes) are estimated using the full covariance matrix. The cell esds are taken into account individually in the estimation of esds in distances, angles and torsion angles; correlations between esds in cell parameters are only used when they are defined by crystal symmetry. An approximate (isotropic) treatment of cell esds is used for estimating esds involving l.s. planes.

Fractional atomic coordinates and isotropic or equivalent isotropic displacement parameters (\AA^2)

	<i>x</i>	<i>y</i>	<i>z</i>	$U_{\text{iso}}^*/U_{\text{eq}}$	Occ. (<1)
Ni1	0.33034 (2)	0.69342 (2)	0.18429 (4)	0.00599 (6)	
Ni2	0.500000	0.87799 (2)	1.000000	0.00683 (7)	
Fe1	0.500000	0.500000	0.000000	0.00327 (9)	
K1	0.40983 (18)	0.500000	0.4730 (2)	0.0200 (3)	0.472
K2	0.38224 (13)	0.90311 (11)	0.48618 (19)	0.0242 (3)	0.417
K3	0.1849 (7)	0.500000	0.4893 (8)	0.0560 (19)	0.192
P1	0.41063 (4)	0.69522 (3)	0.72442 (7)	0.00485 (8)	
P2	0.19569 (6)	0.500000	−0.01061 (10)	0.00557 (11)	
O1	0.31025 (13)	0.70594 (10)	0.8587 (2)	0.0072 (2)	
O2	0.34525 (14)	0.68172 (11)	0.4959 (2)	0.0102 (2)	
O3	0.50488 (13)	0.60977 (10)	0.7970 (2)	0.0069 (2)	
O4	0.50525 (13)	0.78185 (10)	0.7692 (2)	0.0082 (2)	
O5	0.19430 (13)	0.58983 (10)	0.1265 (2)	0.0085 (2)	
O6	0.06136 (18)	0.500000	−0.1681 (3)	0.0087 (3)	
O7	0.30728 (19)	0.500000	−0.1148 (3)	0.0103 (3)	

Atomic displacement parameters (\AA^2)

	U^{11}	U^{22}	U^{33}	U^{12}	U^{13}	U^{23}
Ni1	0.00441 (10)	0.00697 (10)	0.00638 (10)	0.00038 (7)	0.00088 (7)	−0.00015 (7)
Ni2	0.00519 (13)	0.00602 (14)	0.00944 (14)	0.000	0.00207 (10)	0.000
Fe1	0.00218 (18)	0.00293 (18)	0.00478 (19)	0.000	0.00099 (15)	0.000
K1	0.0413 (9)	0.0080 (5)	0.0103 (5)	0.000	0.0055 (5)	0.000
K2	0.0259 (6)	0.0332 (7)	0.0122 (4)	−0.0107 (5)	0.0018 (4)	0.0082 (4)
K3	0.056 (4)	0.100 (6)	0.0100 (17)	0.000	0.005 (2)	0.000
P1	0.00395 (17)	0.00570 (18)	0.00483 (18)	0.00067 (13)	0.00093 (14)	−0.00035 (13)
P2	0.0033 (2)	0.0049 (2)	0.0082 (3)	0.000	0.00071 (19)	0.000
O1	0.0055 (5)	0.0095 (5)	0.0072 (5)	0.0022 (4)	0.0028 (4)	0.0009 (4)
O2	0.0091 (6)	0.0162 (6)	0.0048 (5)	0.0011 (5)	0.0003 (4)	0.0002 (4)
O3	0.0049 (5)	0.0070 (5)	0.0089 (5)	0.0014 (4)	0.0018 (4)	0.0012 (4)
O4	0.0069 (5)	0.0072 (5)	0.0110 (6)	−0.0012 (4)	0.0031 (4)	−0.0022 (4)
O5	0.0071 (5)	0.0067 (5)	0.0120 (6)	−0.0012 (4)	0.0027 (4)	−0.0031 (4)
O6	0.0045 (7)	0.0124 (8)	0.0081 (8)	0.000	−0.0005 (6)	0.000
O7	0.0056 (7)	0.0088 (8)	0.0181 (9)	0.000	0.0060 (7)	0.000

Geometric parameters (\AA , $^\circ$)

Ni1—O2	2.0153 (14)	K1—O7 ^{xi}	3.146 (3)
Ni1—O5	2.0314 (14)	K2—O4	2.631 (2)

Ni1—O1 ⁱ	2.0366 (13)	K2—O6 ^{xii}	2.677 (2)
Ni1—O3 ⁱⁱ	2.0984 (14)	K2—O2 ⁱ	2.737 (2)
Ni1—O1 ⁱⁱⁱ	2.0988 (14)	K2—O5 ⁱ	2.8470 (19)
Ni1—O4 ⁱⁱ	2.1161 (14)	K2—O4 ⁱⁱ	2.851 (2)
Ni2—O4	2.0411 (14)	K2—O6 ^{vi}	2.929 (2)
Ni2—O4 ^{iv}	2.0411 (14)	K2—O1 ⁱ	3.0776 (19)
Ni2—O5 ^v	2.0928 (14)	K2—O7 ^{xii}	3.086 (2)
Ni2—O5 ⁱ	2.0928 (14)	K2—O2	3.149 (2)
Ni2—O6 ⁱ	2.2241 (13)	K3—O7 ^{xi}	2.609 (6)
Ni2—O6 ^{vi}	2.2241 (13)	K3—O5	2.715 (5)
Fe1—O7	2.016 (2)	K3—O5 ^x	2.715 (5)
Fe1—O7 ^{vii}	2.016 (2)	K3—O6 ^{xi}	2.862 (6)
Fe1—O3 ^{viii}	2.0490 (13)	K3—O6 ^{xiii}	2.949 (7)
Fe1—O3 ⁱⁱ	2.0490 (13)	K3—O2	3.077 (4)
Fe1—O3 ^{ix}	2.0490 (13)	K3—O2 ^x	3.077 (4)
Fe1—O3 ⁱⁱⁱ	2.0490 (13)	P1—O2	1.5042 (15)
K1—O3	2.6263 (18)	P1—O1	1.5482 (14)
K1—O3 ^x	2.6264 (18)	P1—O4	1.5679 (14)
K1—O2	2.6673 (16)	P1—O3	1.5694 (14)
K1—O2 ^x	2.6673 (16)	P2—O7	1.509 (2)
K1—O3 ^{ix}	2.6691 (19)	P2—O6	1.554 (2)
K1—O3 ⁱⁱ	2.6691 (19)	P2—O5 ^x	1.5546 (14)
K1—O5	3.091 (2)	P2—O5	1.5546 (14)
K1—O5 ^x	3.091 (2)		
O2—Ni1—O5	90.55 (6)	O3 ^{ix} —K1—O5	93.66 (6)
O2—Ni1—O1 ⁱ	94.23 (6)	O3 ⁱⁱ —K1—O5	65.70 (5)
O5—Ni1—O1 ⁱ	90.23 (6)	O3—K1—O5 ^x	155.60 (8)
O2—Ni1—O3 ⁱⁱ	91.89 (6)	O3 ^x —K1—O5 ^x	115.32 (5)
O5—Ni1—O3 ⁱⁱ	99.19 (5)	O2—K1—O5 ^x	106.12 (6)
O1 ⁱ —Ni1—O3 ⁱⁱ	168.72 (5)	O2 ^x —K1—O5 ^x	59.36 (5)
O2—Ni1—O1 ⁱⁱⁱ	178.70 (6)	O3 ^{ix} —K1—O5 ^x	65.70 (5)
O5—Ni1—O1 ⁱⁱⁱ	88.65 (6)	O3 ⁱⁱ —K1—O5 ^x	93.66 (6)
O1 ⁱ —Ni1—O1 ⁱⁱⁱ	84.74 (6)	O5—K1—O5 ^x	48.38 (6)
O3 ⁱⁱ —Ni1—O1 ⁱⁱⁱ	89.25 (5)	O3—K1—O7 ^{xi}	56.89 (5)
O2—Ni1—O4 ⁱⁱ	92.33 (6)	O3 ^x —K1—O7 ^{xi}	56.89 (5)
O5—Ni1—O4 ⁱⁱ	169.40 (5)	O2—K1—O7 ^{xi}	78.69 (5)
O1 ⁱ —Ni1—O4 ⁱⁱ	99.72 (5)	O2 ^x —K1—O7 ^{xi}	78.69 (5)
O3 ⁱⁱ —Ni1—O4 ⁱⁱ	70.53 (5)	O3 ^{ix} —K1—O7 ^{xi}	144.33 (3)
O1 ⁱⁱⁱ —Ni1—O4 ⁱⁱ	88.64 (5)	O3 ⁱⁱ —K1—O7 ^{xi}	144.33 (3)
O4—Ni2—O4 ^{iv}	96.75 (8)	O5—K1—O7 ^{xi}	106.17 (7)
O4—Ni2—O5 ^v	103.69 (6)	O5 ^x —K1—O7 ^{xi}	106.17 (7)
O4 ^{iv} —Ni2—O5 ^v	92.95 (5)	O4—K2—O6 ^{xii}	135.41 (8)
O4—Ni2—O5 ⁱ	92.95 (5)	O4—K2—O2 ⁱ	89.14 (6)
O4 ^{iv} —Ni2—O5 ⁱ	103.69 (6)	O6 ^{xii} —K2—O2 ⁱ	128.60 (7)
O5 ^v —Ni2—O5 ⁱ	154.96 (8)	O4—K2—O5 ⁱ	66.22 (5)
O4—Ni2—O6 ⁱ	160.71 (6)	O6 ^{xii} —K2—O5 ⁱ	147.28 (7)
O4 ^{iv} —Ni2—O6 ⁱ	94.81 (6)	O2 ⁱ —K2—O5 ⁱ	61.95 (5)

O5 ^v —Ni2—O6 ⁱ	91.06 (6)	O4—K2—O4 ⁱⁱ	79.26 (7)
O5 ⁱ —Ni2—O6 ⁱ	69.28 (6)	O6 ^{xii} —K2—O4 ⁱⁱ	69.19 (5)
O4—Ni2—O6 ^{vi}	94.80 (6)	K2 ^{xiv} —K2—O4 ⁱⁱ	126.86 (4)
O4 ^{iv} —Ni2—O6 ^{vi}	160.71 (6)	O2 ⁱ —K2—O4 ⁱⁱ	105.45 (6)
O5 ^v —Ni2—O6 ^{vi}	69.28 (6)	O5 ⁱ —K2—O4 ⁱⁱ	142.65 (7)
O5 ⁱ —Ni2—O6 ^{vi}	91.06 (6)	O4—K2—O6 ^{vi}	68.58 (5)
O6 ⁱ —Ni2—O6 ^{vi}	78.66 (8)	O6 ^{xii} —K2—O6 ^{vi}	97.82 (7)
O7—Fe1—O7 ^{vii}	180.0	O2 ⁱ —K2—O6 ^{vi}	126.41 (7)
O7—Fe1—O3 ^{viii}	86.58 (5)	O5 ⁱ —K2—O6 ^{vi}	64.47 (5)
O7 ^{vii} —Fe1—O3 ^{viii}	93.42 (5)	O4 ⁱⁱ —K2—O6 ^{vi}	116.35 (6)
O7—Fe1—O3 ⁱⁱ	93.42 (5)	O4—K2—O1 ⁱ	109.01 (6)
O7 ^{vii} —Fe1—O3 ⁱⁱ	86.58 (5)	O6 ^{xii} —K2—O1 ⁱ	85.38 (5)
O3 ^{viii} —Fe1—O3 ⁱⁱ	180.00 (8)	O2 ⁱ —K2—O1 ⁱ	50.84 (4)
O7—Fe1—O3 ^{ix}	93.42 (5)	O5 ⁱ —K2—O1 ⁱ	112.77 (6)
O7 ^{vii} —Fe1—O3 ^{ix}	86.58 (5)	O4 ⁱⁱ —K2—O1 ⁱ	64.63 (5)
O3 ^{viii} —Fe1—O3 ^{ix}	81.87 (8)	O6 ^{vi} —K2—O1 ⁱ	176.79 (6)
O3 ⁱⁱ —Fe1—O3 ^{ix}	98.13 (8)	O4—K2—O7 ^{xii}	165.00 (7)
O7—Fe1—O3 ⁱⁱⁱ	86.58 (5)	O6 ^{xii} —K2—O7 ^{xii}	52.30 (6)
O7 ^{vii} —Fe1—O3 ⁱⁱⁱ	93.42 (5)	O2 ⁱ —K2—O7 ^{xii}	78.76 (5)
O3 ^{viii} —Fe1—O3 ⁱⁱⁱ	98.13 (8)	O5 ⁱ —K2—O7 ^{xii}	114.35 (7)
O3 ⁱⁱ —Fe1—O3 ⁱⁱⁱ	81.87 (8)	O4 ⁱⁱ —K2—O7 ^{xii}	95.32 (5)
O3 ^{ix} —Fe1—O3 ⁱⁱⁱ	180.00 (5)	O6 ^{vi} —K2—O7 ^{xii}	125.92 (6)
O2—P1—O1	110.92 (8)	O1 ⁱ —K2—O7 ^{xii}	56.34 (4)
O2—P1—O4	114.19 (8)	O4—K2—O2	52.08 (5)
O1—P1—O4	108.73 (8)	O6 ^{xii} —K2—O2	125.05 (6)
O2—P1—O3	108.41 (8)	O2 ⁱ —K2—O2	56.55 (6)
O1—P1—O3	112.61 (8)	O5 ⁱ —K2—O2	87.27 (5)
O4—P1—O3	101.72 (8)	O4 ⁱⁱ —K2—O2	59.33 (5)
O7—P2—O6	113.84 (12)	O6 ^{vi} —K2—O2	120.57 (5)
O7—P2—O5 ^x	112.26 (7)	O1 ⁱ —K2—O2	56.94 (4)
O6—P2—O5 ^x	104.37 (7)	O7 ^{xii} —K2—O2	113.14 (5)
O7—P2—O5	112.26 (7)	O7 ^{xi} —K3—O5	139.0 (2)
O6—P2—O5	104.37 (7)	O7 ^{xi} —K3—O5 ^x	139.0 (2)
O5 ^x —P2—O5	109.14 (11)	O5—K3—O5 ^x	55.61 (11)
O3—K1—O3 ^x	72.22 (7)	O7 ^{xi} —K3—O6 ^{xi}	55.72 (11)
O3—K1—O2	56.19 (4)	O5—K3—O6 ^{xi}	143.7 (2)
O3 ^x —K1—O2	125.17 (6)	O5 ^x —K3—O6 ^{xi}	143.7 (2)
O3—K1—O2 ^x	125.17 (6)	O7 ^{xi} —K3—O6 ^{xiii}	149.1 (3)
O3 ^x —K1—O2 ^x	56.19 (4)	O5—K3—O6 ^{xiii}	65.77 (12)
O2—K1—O2 ^x	147.77 (10)	O5 ^x —K3—O6 ^{xiii}	65.77 (12)
O3—K1—O3 ^{ix}	138.56 (8)	O6 ^{xi} —K3—O6 ^{xiii}	93.4 (2)
O3 ^x —K1—O3 ^{ix}	93.79 (6)	O7 ^{xi} —K3—O2	80.84 (14)
O2—K1—O3 ^{ix}	136.75 (7)	O5—K3—O2	59.12 (9)
O2 ^x —K1—O3 ^{ix}	67.30 (4)	O5 ^x —K3—O2	105.29 (19)
O3—K1—O3 ⁱⁱ	93.79 (6)	O6 ^{xi} —K3—O2	110.40 (11)
O3 ^x —K1—O3 ⁱⁱ	138.56 (8)	O6 ^{xiii} —K3—O2	114.13 (11)
O2—K1—O3 ⁱⁱ	67.30 (4)	O7 ^{xi} —K3—O2 ^x	80.84 (14)
O2 ^x —K1—O3 ⁱⁱ	136.75 (7)	O5—K3—O2 ^x	105.29 (19)

O3 ^{ix} —K1—O3 ⁱⁱ	70.89 (7)	O5 ^x —K3—O2 ^x	59.12 (9)
O3—K1—O5	115.32 (5)	O6 ^{xi} —K3—O2 ^x	110.40 (11)
O3 ^x —K1—O5	155.60 (8)	O6 ^{xiii} —K3—O2 ^x	114.13 (11)
O2—K1—O5	59.36 (5)	O2—K3—O2 ^x	112.8 (2)
O2 ^x —K1—O5	106.12 (6)		

Symmetry codes: (i) $-x+1/2, -y+3/2, -z+1$; (ii) $-x+1, y, -z+1$; (iii) $x, y, z-1$; (iv) $-x+1, y, -z+2$; (v) $x+1/2, -y+3/2, z+1$; (vi) $x+1/2, y+1/2, z+1$; (vii) $-x+1, -y+1, -z$; (viii) $x, -y+1, z-1$; (ix) $-x+1, -y+1, -z+1$; (x) $x, -y+1, z$; (xi) $x, y, z+1$; (xii) $-x+1/2, -y+3/2, -z$; (xiii) $-x, -y+1, -z$; (xiv) $x, -y+2, z$.